

Article

# Plasma Polymerization SnOxCy Organic-like Films and Grafted PNIPAAm Composite Hydrogel with Nanogold Particles for Promotion Thermal Resistive Properties

Running title: Plasma Polymerization to Improve Thermal Resistive Properties

Chin-Yen Chou <sup>1</sup>, Ko-Shao Chen <sup>1</sup>, Win-Li Lin <sup>2</sup>, Ying-Cian Ye <sup>3</sup> and Shu-Chuan Liao <sup>2,3,\*</sup>

<sup>1</sup> Department of Materials Engineering, Tatung University, Taipei 104, Taiwan; smy0215@msn.com (C.-Y.C.); kschen@ttu.edu.tw (K.-S.C.)

<sup>2</sup> Institute of Biomedical Engineering, National Taiwan University, Taipei 106, Taiwan; winli@ntu.edu.tw

<sup>3</sup> Bachelor Program for Design and Materials for Medical Equipment and Devices, Da Yeh University, Changhua 515, Taiwan; an501290294@gmail.com

\* Correspondence: liaozizi@mail.dyu.edu.tw; Tel.: +886-4-851-1888 (ext. 2622); Fax: +886-4-8511666

**Abstract:** In this study, a new type of temperature sensor device was developed. The circular electrode of the thermal sensitive sensor was modified with TMT and O<sub>2</sub> plasma to enhance the conductivity by forming a thin SnOxCy layer on the electrode surface. The Nano-Au particles were subjected to O<sub>2</sub> plasma pretreatment to form peroxide groups on the surface. The thermally sensitive sensor was made by mixing the above-treated Nano-Au particles with N-isopropylacrylamide (NIPAAm) to form solution and then UV-induced grafting polymerization of the NIPAAm-containing solution onto the electrode substrate. The composite hydrogels on the electrode introduce thermo-sensitive polymeric surface films for temperature sensing. Using ambient environment resistance test to measure the resistance, the LCST (lower critical solution temperature) of Nano-Au (MUA) mixed with NIPAAm hydrogel was found to be 32 °C. At ambient temperatures higher than LCST, the electrode resistance decreases linearly.

**Keywords:** nano-Au particles; NIPAAm hydrogel; plasma treatment; UV grafting

---

## 1. Introduction

There are many types of commercially available temperature sensor elements such as thermistors, resistance type temperature sensors, thermal couples and temperature-sensing IC etc. The advantages of resistance type temperature sensors are high linearity, wide linear range, high output signal level and accuracy, but the disadvantage is necessity to have three or four wired circuit, bulky components, slow conduction and response. Thus, it is not suitable for rapid temperature measurement as well as for smaller objects.

P (NIPAAm) is a well-known thermo-responsive polymer and exhibits a lower critical solution temperature (LCST) of about 32 °C in an aqueous medium. It assumes a random coil structure (hydrophilic state) below the LCST and a collapsed globular structure (hydrophobic state) above the LCST [1]. Using UV light, Peng and Cheng (1998) grafted NIPAAm onto porous polyethylene membrane. They noted that the temperature-responsive behavior of the grafted membranes changes with the grafting level. NIPAAm was also successfully grafted onto track membranes made of PC (Park et al., 1998; Xie et al., 2005), PET (Shtanko et al., 2000; Reber et al., 2001), PP (Shtanko et al., 2000) and poly(vinylidene fluoride) (PVDF) (Mazzei et al., 2000) [2].

Because of the reversible phase transition, P (NIPAAm) has been used in the synthesis of thermal sensitive hydrogels. P(NIPAAm)-based hydrogels absorb water and exist in swollen states below the LCST. However, they undergo an abrupt and drastic shrinkage in volume as the medium temperature is raised above the LCST. These unique characteristics allowed the P(NIPAAm)-based

hydrogels use in biomedical applications, such as in the controlled release of drugs and in tissue engineering. Furthermore, its phase transition behavior can be controlled by incorporating more hydrophilic or hydrophobic monomer in the gel composition [3].

It is well known that plasma treatment can alter the physical-chemical properties of a polymer surface. Improvements such as wettability, permeability, conductivity, printability, adhesion or biocompatibility can be easily achieved using plasma treatment in a very short time. The main reactions during plasma treatment on polymer surface are etching, cleaning, crosslinking, grafting and other chemical reactions depending on the presence of active species in plasma [4]. The plasma deposition of TMT ( $\text{Sn}(\text{CH}_3)_4$ ) has been found to conduce to materials with useful antistatic coatings. This is because of their interesting gas sensing properties that have been widely applied to thin or thick film devices, flat display devices, transparent electrodes, anti-static films, thin film resistors and heat reflectors [5-11]

Nano-Au particles is a suspension (or colloid) of sub-micrometre-sized particles of gold in a fluid, usually water. The liquid is usually either an intense red color (for particles less than 100 nm), or a dark yellowish color (for larger particles). Due to the unique optical, electronic, and molecular-recognition properties of gold nanoparticles, they are the subject of substantial research, with applications in a wide variety of areas, including electron microscopy, electronics, nanotechnology, and materials science. [12-13]

## 2. Experimental Details

### 2.1 Preparation of circular electrode and glass

The structure of circular electrode used is shown in Fig.2. It was made by screen-printing silver paste on the alumina substrate and then sintering. This kind of electrode has advantages of low point discharge and large effective area, so it promotes measurement sensitivity and decreases the loss of signal from point discharge.

The slide glass and circular electrode were cut into size of  $1 \times 1 \text{ mm}^2$ . The substrate electrodes were then cleaned ultrasonically in 95% ethyl alcohol solvent and distilled water for 15 min and dried in desiccators to remove the surface contaminants and organic matters. This would ensure a good adhesion between the substrate and the deposited films [14-16]. This study used radio frequency (RF) oxygen plasma treatment as a process for the polymeric substance to be grafted onto the substrate. A new type temperature sensor was successfully produced by UV-induced graft polymerization of NIPAAm monomer onto nano-Au particles and then immobilization of grafted nano-Au particles onto the electrode substrate. It combines the advantages of electrical conductivity of nano-Au particles with temperature sensibility of NIPAAm hydrogel. This new composite device is small in dimension, fast in response, lower cost in fabrication, high stability in practical usage, and can improve the disadvantage of common resistance type temperature sensors. The experimental flow chart of this study is shown in Fig. 1

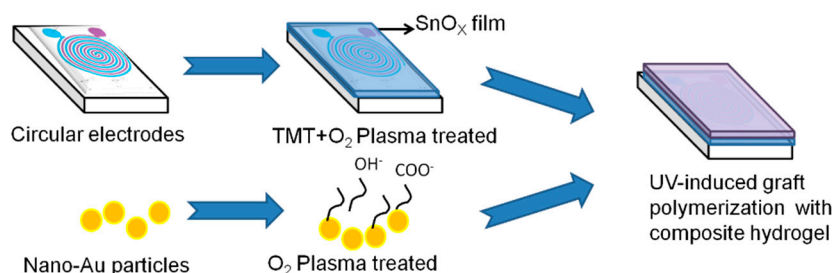


Fig. 1 Flow chart of this study.

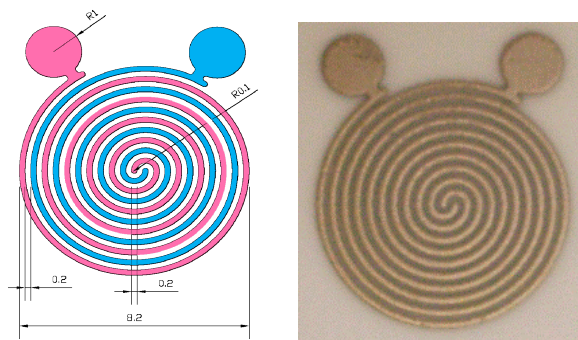


Fig. 2 The structure of circular electrode (size:  $1 \times 1 \text{ cm}^2$ ).

### 2.2 Plasma pre-treatment

Gold nanoparticles (Nano-Au) were obtained by reducing trisodium citrate and hydrogen tetrachloroaurate(III) tetrahydrate (chloroauric acid) and modifying with 11- mercaptoundecanoic acid (MUA) by the self-assembly monolayers (SAM) [17]. The Nano-Au particles were subjected to  $\text{O}_2$  plasma pretreatment to form peroxide groups on the surface. The plasma polymerization system mainly comprises a bell-jar reaction chamber and 13.56 MHz radio frequency generators (model OEM-6 POWER SYSTEMS, eni Co) [18]. Nano-Au particles (concentration: 1.5 ml, 3.0 ml, and 4.5ml dried in  $40^\circ\text{C}$ ) were first subjected to oxygen plasma treatment to activate groups ( $\text{OH}$ ,  $\text{COO}^-$ ) on the particle surface. The  $\text{O}_2$  plasma treatment was operated at 100 W, 40 mtorr for 1min. In oxygen plasma treatment, two processes may occur: etching of the polymer surface through the reactions of atomic oxygen with the surface carbon atoms to produce volatile reaction products, and the formation of oxygen functional groups at the surface through the reactions between the active species from the plasma and the surface. The balance of these two processes depends on the operation parameters of a given experiment.

Prior to immobilization by nano-Au particles to the circular electrode, the circular electrode was modified with TMT and  $\text{O}_2$  plasma to enhance conductivity by forming a layer of  $\text{SnO}_x\text{C}_y$  film on the surface. The chamber was pumped down to a base pressure of 30 mTorr before introducing mixtures of TMT ( $\text{Sn}(\text{CH}_3)_4$ , purity >99%, vacuum degassed) and oxygen gas (purity >99%). Deposition was performed at an input power of 100 W, deposition time of 10min, and TMT/ $\text{O}_2$  ratio of 40:40 in mTorr.

### 2.3 Post treatment by photo UV-induced grafting polymerization

The Schematic diagram of UV-light (Sunshine Inc. ,R.O.C) system [19]. The electrode substrates after plasma treatment were immersed into the different nano-Au concentration (1.5 ml, 3.0 ml, and 4.5 ml) and NIPAAm monomer mixture solution in Pyrex glass utensil. The glass utensil was sealed and then irradiated with UV light (wavelength= $365\text{nm}^{-1}$ ) at 2000 W for 15 min to induce grafting polymerization.

### 2.4 Characterization

#### Surface contact angles

The water contact angles (WCA) of the untreated and the subsequent deposited films were measured by the sessile drop (0.2–0.3 ml) method with distilled water by a syringe and observed by CCD at room temperature ( $25.0^\circ\text{C}$ ) (Goni-meter type G-1 made by ERMA Optical Works Co. LTD). The drop image was recorded by a video camera. The measured WCA value was the average of three measurements.

## Morphology

The surface morphology of plasma deposited films was observation of scanning electron microscope (JEOL, JSM-5600). The samples were placed on aluminum or copper holder and sputtering coated with a thin layer of gold (coating 90 seconds) to improve the electrical conductivity.

## UV-VIS spectra

Ultraviolet-visible spectroscopy (Jasco V-560, 300 nm - 800 nm) refers to absorption spectroscopy in the ultraviolet-visible spectral region. The absorption or reflectance in the visible range directly affects the perceived color of the chemicals involved. In this study, calibration was determined from the relation between nano-Au particles concentrations and UV-VIS specific wavelength (525.5nm) intensity. Through this way, the distribution of nano-Au in NIPAAm solution could be obtained with high accuracy.

## Resistance measurement

The resistance of electrode was measured by Keithley 2000. The output/input terminals of electrodes were first connected to the equipment and kept in the dry air until the signal was stable. The electrode was then soaked in the deionized water in a heat-resistance glass container, and the deionized water was heated to the temperature of 45.0 °C. The resistance was recorded per 15 seconds to a precision of 1 degree.

## 3. Results and Discussions

### 3.1 Resistance and Surface contact angles

The values of circular electrode resistance after different treatment are listed in Table 1. The resistance of pure nano-Au solution is 11.9 k $\Omega$ , while that of TMT+O<sub>2</sub> treated electrode is 20.8 k $\Omega$ . Because of the low conductivity of NIPAAm hydrogel, the resistance increases to 130 k $\Omega$  after immobilization of NIPAAm hydrogel on the circular electrode. From table.1, it clearly indicates that with increase in the treated nano particles, the resistance of composite hydrogel decreases (from 130 k $\Omega$  to 60.4 k $\Omega$ ) due to the excellent conductivity of nano-gold particles. The concentration of nano particles in composite hydrogel improves the conductivity of the circular electrode.

**Table.1** Values of the circular electrode resistance after different treatment.

	Nano-Au solution	treatment A	treatment B	treatment C	treatment D	treatment E
Resistance (K $\Omega$ )	11.9 $\pm$ 2.3	20.8 $\pm$ 2.2	130 $\pm$ 5.5	59.2 $\pm$ 3.4	61.5 $\pm$ 4.9	60.6 $\pm$ 2.9

Treatment A- TMT&O<sub>2</sub> plasma treatment, treatment B- Hydrogel with 0 ml Nano-Au particles, treatment C- Hydrogel with 1.5 ml Nano-Au particles, treatment D- Hydrogel with 3.0 ml Nano-Au particles, and treatment E- Hydrogel with 4.5 ml Nano-Au particles

The values of water contact angle (WCA) of electrode substrate after each treatment are listed in table.2. The WCA of glass substrate after TMT+O<sub>2</sub> treatment decreases from the untreated substrate (40.1°) to less than 10°, exhibiting hydrophilic property. The WCA increases to 41.0° by the immobilization of NIPAAm hydrogel on the substrate surface. The time for completing absorption of water by the NIPAAm hydrogel takes about 100 seconds. After the absorption by distilled water, the measured WCA decreases again to less than 10°. This illustrates that the absorption time of hydrogel may affect the sensitivity and stability of the composite hydrogel sensor. The effect of soaking time on the resistance of electrode will be discussed later in this work.

**Table.2** Water contact angles of electrode substrate after different treatment

	Untreated	treatment A	treatment B	treatment C	treatment D	treatment E
$\theta_{H_2O}$	40.1°	<10°	41.0	31.5	43.2	43.1

Treatment A- TMT&O<sub>2</sub> plasma treatment, treatment B- Hydrogel with 0 ml Nano-Au particles, treatment C- Hydrogel with 1.5 ml Nano-Au particles, treatment D- Hydrogel with 3.0 ml Nano-Au particles, and treatment E- Hydrogel with 4.5 ml Nano-Au particles

### 3.2 Environmental test

The variations of electrode resistance as well as hydrogel mass with soaking time at 25 °C is shown in Fig.3. At the initial 100 seconds, NIPAAm hydrogel absorbs most deionized water therefore exhibits a drastic resistance drop. However with further increased soaking time, the resistance decreases in a slow rate as reflected from the small slope, indicating that hydrogel becomes saturation when soaking period is more than 100 seconds, thus no significant variation of resistance upon the soaking time.

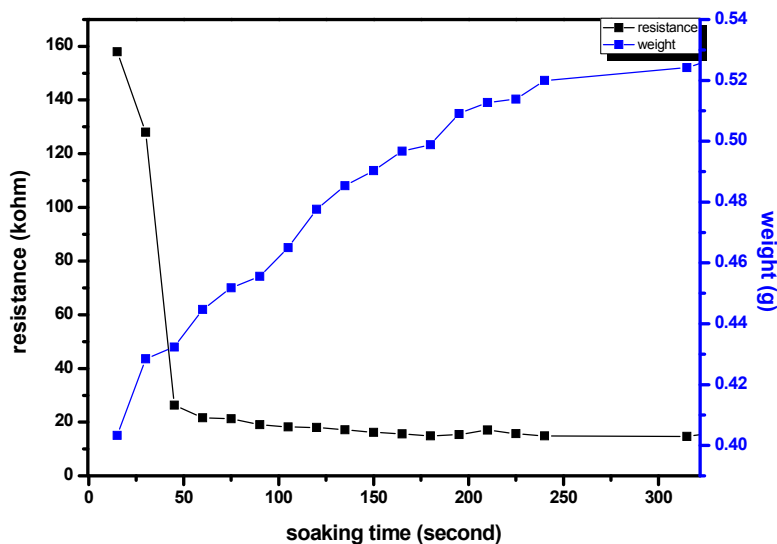


**Fig. 3** Variations of electrode resistance as well as hydrogel mass with soaking time.

Fig. 4 shows tendency of resistance upon the temperature for specimen with different amount of nano-Au particle. Being soaked in water for 100 seconds, these samples are slowly heated from 25 °C to 45 °C. The resistance is recorded accordingly as temperature increases by each degree. As seen in fig. 4, the resistance drops linearly with increased temperature. The fitted curve slopes of specimen with 0ml, 1.5ml, and 3.0ml nano-Au are -0.84, -2.30, and -1.22 respectively. It should be pointed out that when temperature is higher than 31 °C, the composite hydrogel becomes globular collapsed structure and causes the nano-Au particles contact with electrode surface. When temperature is lower than 31 °C, the structure of NIPAAm becomes unfolded. The morphological changes in NIPAAm hydrogel structure are illustrated in fig.5.

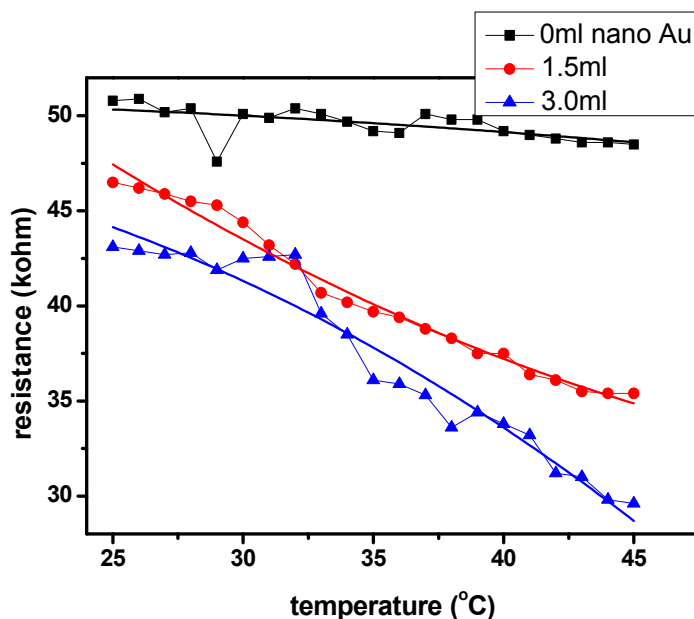


Fig.4 Variations of resistance with temperature for two samples.

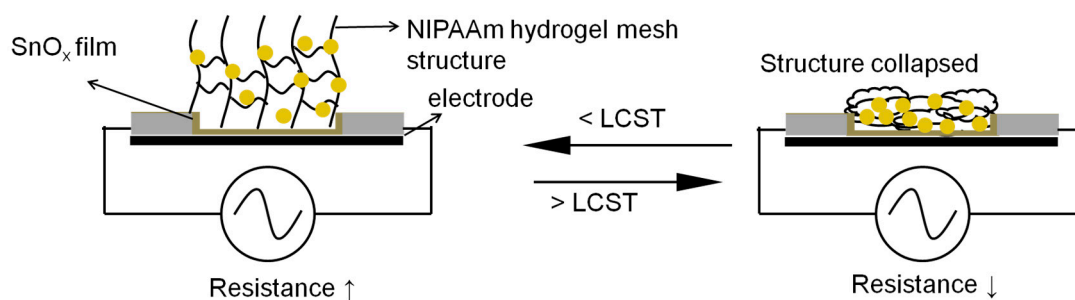
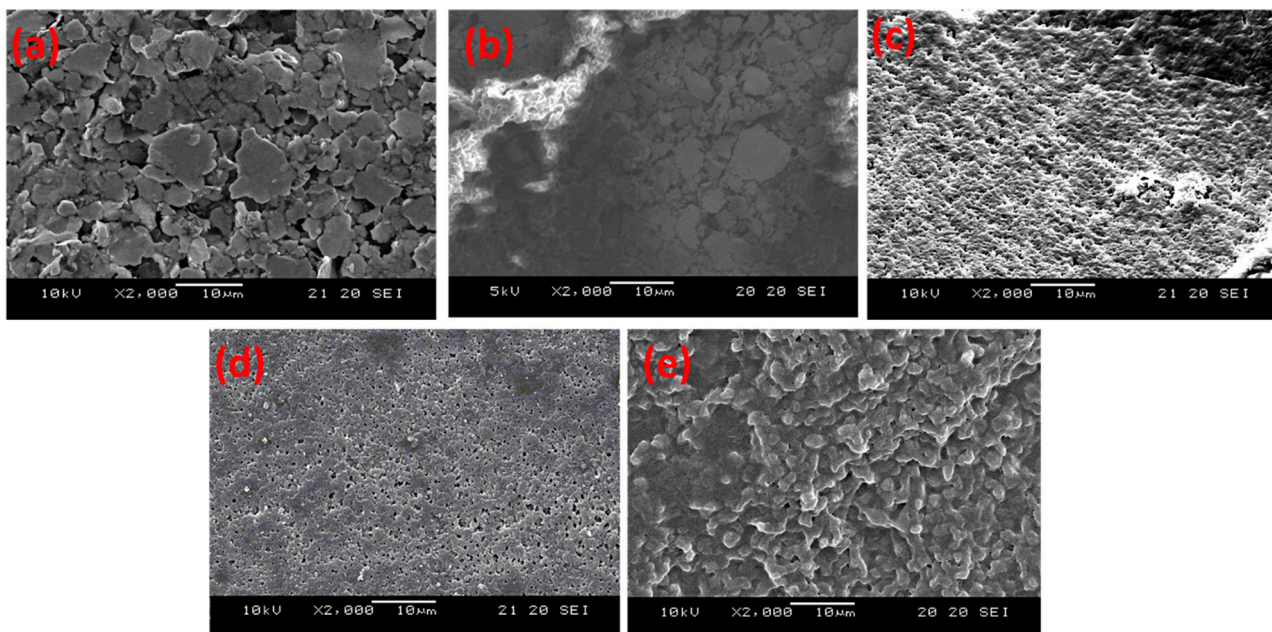


Fig.5 Morphological changes in NIPAAm hydrogel structure.

### 3.3 SEM morphology

The SEM morphologies of the samples after various treatments are shown in Fig.6. Fig.6 (a) shows the surface of untreated electrode. After grafting with NIPAAm hydrogel only, the electrode surface is covered with a homogeneous hydrogel layer and the surface roughness is small (Fig.6 (b)). Figs. 6 (c) to 6(e) demonstrates the electrode surface with grafted hydrogels in amount of 1.5 ml, 3.0 ml, and 4.5ml nano-Au, respectively. The surfaces on these figures are rough with a large number of pores as compared to the image in Fig. 6(b). The pore structure is believed to provide more contact area thus can enhance the sensitivity of sensor. In particular, samples with 1.5 ml and 3 ml nano-Au exhibit the largest number of pores per area on the surface.



**Fig.6** SEM morphologies of (a) untreated sample, and composite gels containing (b) 0 ml, (c) 1.5 ml, and (d) 3.0 ml and (e) 4.5 ml nano-Au particles. (2000x)

### 3.4 UV-VIS spectra

To evaluate the distribution of nano-Au particles in NIPAAm solution, UV-VIS was used to detect the intensity of specific absorption peak at 525.5nm. Fig.7 shows the UV-VIS spectra of nano-Au particles of different concentration as well as the calibration curve. The slope of calibration curve is 0.99, indicating that particles are uniformly distributed in the NIPAAm solution. From the calibration curve and ZETA potential analysis, the concentration of nano-Au particles is found to be  $1.07 \times 10^{13}$  (particles/ml) and the particles average size is  $15.6 \pm 2.7$ nm.

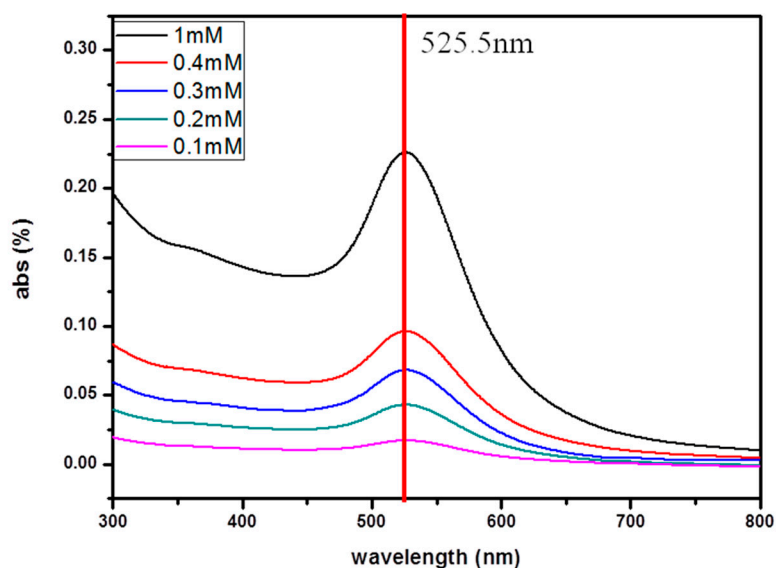


**Fig.7** UV-VIS spectra of nano-Au particles in different concentration and the corresponding calibration curve.

### 3.5 Response and Recovery test

The response of composite sensors is estimated by measuring the variation of resistance with time at temperatures between 25 °C and 45 °C over a period of 2 minutes and the results of composite sensors containing 1.5 ml, 3.0 ml, and 4.5ml of nano-Au particles are shown in fig.8. This figure indicates that 1.5 ml nano-Au addition to the hydrogel is the best with resistance decrease from 45.5 kΩ to 35.4kΩ in 1 second and has the highest sensitivity of 0.39. Furthermore, the result shows that both the response time and recovery time are short. Compared to control sample, NIPAAm hydrogels with nano-Au particles addition enhance the sensitivity and stability of temperature detection.

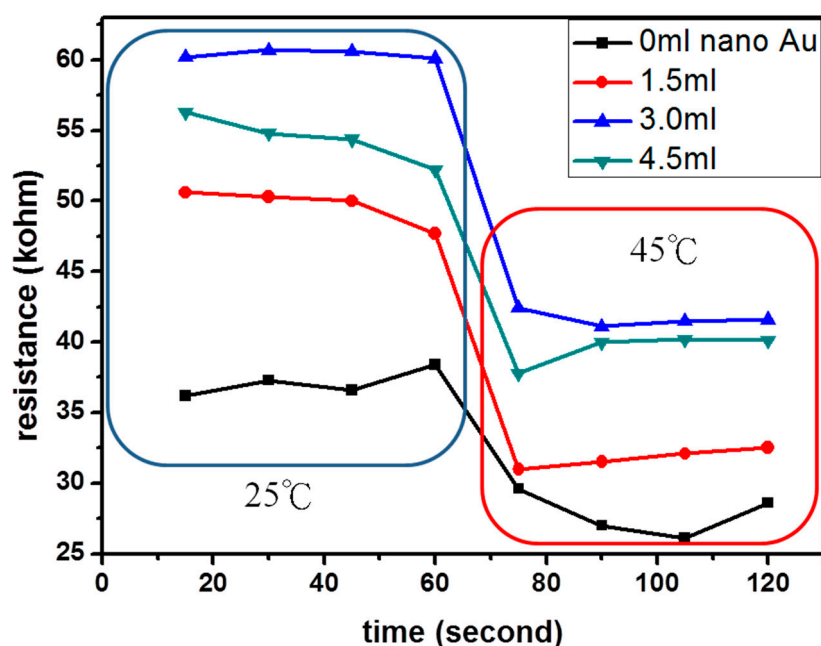


Fig.8 Sensor response of sensor devices containing (a) 0 ml, (b) 1.5 ml, (c) 3.0 mg, and (d) 4.5 ml nano-Au particles between 25 °C and 45 °C over a period of 2 minutes.

## 4. Summary

In this study, nano-Au particles with NIPAAm hydrogel was successfully grafted on the electrode surface to form composite hydrogel for temperature sensing. Using ambient environment resistance test to measure the resistance variation of the sensor, it was found that the resistance drops linearly with increased temperature due to the collapse of NIPAAm hydrogel to globular shape. When the environment temperature is below 31 °C, NIPAAm hydrogel swells up and causes increase in resistance. This change in NIPAAm structure is a reversible reaction so that the sensor can be reusable. From the calibration curve and ZETA potential analysis, the concentration of nano-Au particles is found to be  $1.07 \times 10^{13}$  (particles/ml) and the particles average size is  $15.6 \pm 2.7$  nm. The stability for samples with 1.5ml nano-Au particle addition is the best with sensitivity of 0.39.

## Reference and Notes

- [1] E.T Kang, *Biomaterials* 27: 2787–2797, 2006.
- [2] Qi Liu, Zhiyong Zhu, *Radiation Physics and Chemistry* 76 :707–713, 2007.
- [3] C.S. Cho, *Polymer* 41:5713–5719, 2000.
- [4] Y.M Chung, *Surface and Coatings Technology* 174 –175:1038–1042, 2003.
- [5] V. Krivetsky *Procedia, Chemistry* 1: 204–207, 2009.
- [6] Zdenek Remes, *Thin solid Films* 23: 6287–6289, 2009.
- [7] Joop van Deelen, *Energy Procedia* 2: 41–48, 2010.
- [8] J. Janca *Surface and Coatings Technology*, 98: 851–854, 1998.
- [9] Vinay Gupta, *Sensors and Actuators B* 156: 743–752, 2011

- [10] Hui Huang, *Sensors and Actuators B* 138: 201–206, 2009.
- [11] Sutichai Chaistsk, *Sensors* 11: 7127-7140, 2011
- [12] Bernhard Wessling, *Conductive Polymer / Solvent Systems: Solutions or Dispersions?*, 1996
- [13] Paul Mulvaney, University of Melbourne, *The beauty and elegance of Nanocrystals*,
- [14] KS Chen, HM Wu, HR Lin, SC Liao, TC Hung, HC Lin, TY Chia, *Biomed Eng Appl Basis Comm*, 21:371-374, 2009.
- [15] KS Chen, MS. Li, HM Wu, MR Yang, JY. Tian, FY Huang, HY Hung, *Surface & Coatings Technology*, 200: 3270 – 3277, 2006.
- [16] E.Kny, *Thin solid Films* 85:23, 1981.
- [17] Ko-Shao Chen\*, Tsui-Shan Hung, Hsin-Ming Wu, Jen-Yuan Wu, Ming-Tse Lin, and Chi-Kuang Feng, *Thin Solid Films* 518: 7568-7573, Sep. 2010
- [18] Shu-Chuan Liao, Hsin-Ming Wu, Yu-Chia Tsao, Hong-Ru Lin, and Ko-Shao Chen\*, *Journal of Nanoscience and Nanotechnology* 12: 1-4, 2012
- [19] Ko-Shao Chen\*, Shu-Chuan Liao, Shen-Wei Lin, Tsui-Shan Hung, Shao-Hsuan Tsao, Hsin-Ming Wu, Norihiro Inagaki, and Wei-Yu Chen, *Japanese Journal of Applied Physics* 51:01AJ06, Jan. 2012



© 2016 by the authors; licensee *Preprints*, Basel, Switzerland. This article is an open access article distributed under the terms and conditions of the Creative Commons by Attribution (CC-BY) license (<http://creativecommons.org/licenses/by/4.0/>).